Fusion Engineering and Design 169 (2021) 112441

Contents lists available at ScienceDirect

Fusion Engineering and Design

journal homepage: www.elsevier.com/locate/fusengdes

The T-containment properties of a Zr-containing Li rod in a high-temperature gas-cooled reactor as a T production device for fusion reactors

Hideaki Matsuura [a,*], Takuro Suganuma [a], Yuki Koga [a], Motomasa Naoi [a], Kazunari Katayama [b], Teppei Otsuka [c], Minoru Goto [d], Shigeaki Nakagawa [d], Shinpei Hamamoto [d], Etsuo Ishitsuka [d], Kenji Tobita [e], Satoshi Konishi [f], Ryoji Hiwatari [g], Youji Someya [g], Yoshiteru Sakamoto [g]

[a] Dept. Applied Quantum Phys. Nucl. Eng., Kyushu Univ., 744 Motooka, Fukuoka 819-0395, Japan
[b] Dept. Advanced Energy Eng. Sci., Kyushu Univ., 6-1 Kasugakouen, Kasuga City, Fukuoka 816-0811, Japan
[c] Dept. Electrical and Electronic Eng., Kindai Univ., 3-4-1 Kowakae, Higashi-Osaka City, Osaka 577-0818, Japan
[d] Japan Atomic Energy Agency, 4002 Narita-cho, Oarai-machi, Higashi-Ibaraki-gun, Ibaraki 311-1393, Japan
[e] Dept. Quantum Sci. Energy Eng., Tohoku University, 6-6-01-2 Aoba, Sendai City, Miyagi 980-8579, Japan
[f] Institute for Advanced Energy, Kyoto University, Gokasho, Uji, Kyoto 611-0011, Japan
[g] National Institutes for Quantum and Radiological Sci. Tech., Rokkasho, Aomori 039-3212, Japan

ARTICLE INFO

Keywords:
Tritium
Zirconium
Nickel coating
Lithium-Loading rod
HTTR
GTHTR300
DEMO fusion reactor

ABSTRACT

The production of tritium (T) using high-temperature gas-cooled reactors (HTGRs) has been studied for a prior engineering research with T handling and initial T possession in demonstration fusion reactors. Stable containment of T in Li-loading rods during HTGR operation is a critical issue. This study investigates this for an irradiation test to examine T-containment performance in Li-loading rods and develops an analytical model of evaluating the amount of T outflow to a He coolant. The hydrogen absorption characteristics, including the deterioration of the hydrogen absorption speed after Zr has sufficiently absorbed the hydrogen, is experimentally measured assuming an HTGR setting. We present an analytical model of evaluating the T outflow from a Li rod and, on the basis of this model, estimate the total T outflow, assuming the presence of a gas-turbine high-temperature reactor of 300 MWe with a nominal capacity and a high-temperature engineering test reactor. It is demonstrated that, by loading a sufficient amount of Zr into the Li rod, the T outflow can be suppressed to less than a small percent of the total T produced during 360 days of reactor operation.

1. Introduction

In technical tests of tritium (T) circulation and initial T possession in a demonstration (DEMO) fusion reactor, it is important to prepare the T-supply method using an outside source [1]. The T has often been produced by means of a D(n,γ)T reaction in Canadian Deuterium Uranium (CANDU) reactors [2]; however, uncertainties in the T-supply scenario in the case of DEMO reactors seem to be continuing to increase. Because the cross-section of the ^{6}Li(n,α)T reaction is almost six orders of magnitude larger across the thermal-neutron energy range compared with the D(n,γ)T reaction in CANDU reactors, and high-temperature gas-cooled reactors (HTGRs) have several advantages (outlined below), we use an HTGR [3] to analyze T production by inserting a Li compound as a burnable poison (BP) instead of a boron compound. The main core structure in an HTGR is graphite, which is chemically stable and does not react with the Li compound. Although the large core size of an HTGR is not attractive from an economic viewpoint, it provides enough space for loading the Li compound without ^{6}Li enrichment, along with structural materials to prevent leakage of T. In an HTGR, the BP is typically inserted in a solid state (i.e., as B_4C), separately from the fuel component; therefore, the Li compound can be loaded into the reactor's core without significantly changing the original structural design. This treatment is efficient in terms of both (1) the increment of available BP for T production and (2) T recovery. The nuclear characteristics and fuel temperature condition were analyzed to confirm the nuclear and thermal feasibility of a lithium (Li)-loaded HTGR [4], and it

* Corresponding author.
E-mail address: matsuura@kyudai.jp (H. Matsuura).

https://doi.org/10.1016/j.fusengdes.2021.112441
Received 1 November 2020; Received in revised form 14 February 2021; Accepted 1 March 2021

is demonstrated that the analysis results satisfy the design requirements. Therefore, the nuclear and thermal feasibility of a Li-loaded HTGR that produces thermal energy and T was confirmed [4].

At this stage, we are aiming for compatibility between electricity and T production in an HTGR. We currently consider that the amount of T flowing out from Li rods to form helium gas should be suppressed to a lower level during operating periods. We investigate the Li-loading rod structure to contain T using dense quality Al_2O_3. Numerical simulations have predicted that if we can operate the HTGR in a low-temperature range, keeping the rod temperature below 500 °C, the leakage of T from the Li rod with the Al_2O_3 layer can be suppressed to less than 1% of the total amount produced [5]. However, if we intended to operate the HTGR in a much higher temperature range (i.e., the rod temperature reaching ~900 °C) to improve the electricity generation efficiency, the T permeability of the Al_2O_3 layer in the Li rod would increase [6], and the leakage of the T would rapidly increase. To reduce the outflow of the T during such an operation, we attempt to adopt Zr in the rod as a T absorption material to avoid increasing the inner T partial pressure [7–11]. The T pressure in the Li rod during HTGR operation could be determined by the pressure balance between the production rate, absorption by Zr, and outflow rates from the rod. The T production rate can be estimated using the neutron flux in the reactor core, which is evaluated by the neutron transport and nuclear burning analyses; the T absorption is governed by the properties of the Zr. The T outflow rate can be estimated from diffusion theory with respect to the Al_2O_3 layer, which depends on the T pressure itself. If we could keep the T pressure at a lower level during the reactor operation period, the T outflow would also be suppressed to a lower level. It is well known that the T absorption property of Zr depends on the preabsorbed (contained) T state in the Zr. This property is also affected by the oxidation of the surface area. It is important to specify the deterioration of the hydrogen absorption rate in Zr under the HTGR conditions during operation. For development of an irradiation test in the HTGR, a tentative analysis model is required.

In this study, we experimentally measure the basic hydrogen absorption properties of Zr in an HTGR setting and estimate the T outflow ratio from the Li-loading rod to the He coolant, assuming the 300 MWe gas-turbine high-temperature reactor (GTHTR300) and high-temperature engineering test reactor (HTTR) to be operating at nominal capacity [12,13].

2. Experimental apparatus and analysis model

2.1. Hydrogen absorption experiment

Hydrogen absorption experiments were carried out using a Zr cylinder (see Table 1) with a diameter of 15.8 mm and a height of 15 mm (1 mm thickness). A schematic illustration of the experimental apparatus is presented in Fig. 1. A Zr cylinder was introduced in the center region of a quartz tube, which was heated to the preset temperature of 900 °C; this temperature was kept constant during the measurement procedures. To control the hydrogen inlet speed, a mass-flow controller was introduced. After the inside of the quartz tube had been evacuated, hydrogen gas flowed into the tube controlling the inlet speed. After the inner hydrogen pressure reached the target values, the hydrogen inflow was halted. The pressure increments during hydrogen inflow and reduction after termination with hydrogen absorption by Zr were continuously observed.

Table 1
Properties of Zr.

Impurity	
C (wt%)	0.015
FeCr (wt%)	0.083
H (wt%)	<0.0003
N (wt%)	0.006
O (wt%)	0.143
Zr+Hf (wt%)	99.5

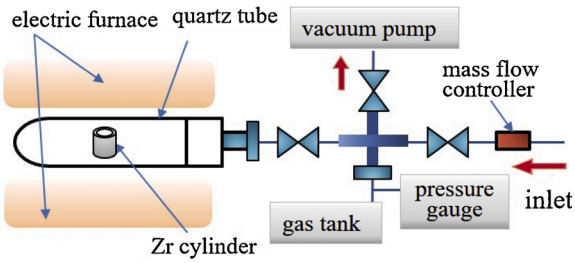

Fig. 1. Illustration of the experimental apparatus.

2.2. Neutron transport and nuclear burning simulation for GTHTR300 and HTTR cores

The estimations of the amount of produced T (production rate) and the effective multiplication factor during the GTHTR300 and HTTR operations were made using the continuous-energy Monte Carlo transport code, MVP-BURN [14], which used the entire core model. Throughout the calculations, nuclear data were taken from JENDL-4.0 [15]. The fuel region temperature was 1,100 °C, and the Li rod temperature was the same as that of the moderator (900 °C).

Fig. 2(a) presents a horizontal cross-section of a gas-turbine high-temperature reactor with a 300 MWe nominal capacity (GTHTR300) core [12]. The core consists of 90 fuel columns arranged in an annular ring; 55 inner and 36 outer removable reflector columns; 18 inner and 12 outer control rod guiding columns; and 8 outer fixed reflector sectors. Each fuel column was composed of eight hexagonal graphite blocks, which were piled up vertically. The hexagonal fuel block was 407 mm wide across the flats (including 1 mm gaps on both sides) and 1,000 mm high, with arrays of 57 fuel channels and 3 BP insertion holes (see Fig. 2 (b)). The fuel rod placed in the fuel channel was enclosed in a graphite block and comprised fuel compacts and a graphite sleeve of a 26 mm diameter. The diameter of each fuel channel in the fuel block was 39 mm, and helium gas flowed through the space between the walls of the fuel channel and a fuel rod as a coolant.

The horizontal cross-section of the HTTR core is also illustrated in Fig. 3(a) [13]. The core consists of two regions, namely the actual core and reflector regions. The actual core consisted of 30 fuel and 7 control rod guide columns, each of which was composed of a stack of 5 fuel and 4 reflector blocks. The actual core was surrounded by the reflector region, i.e., replaceable and permanent reflector blocks and 9 control rod guide blocks. The core was 2.9 m in height and 2.3 m in diameter. Each hexagonal block was 360 mm wide across the flats and 580 mm high [see Fig. 3(b)]. The fuel block contained 31 or 33 fuel channels and 3 BP insertion holes. Li rods that were 480 mm high with 15 mm Al_2O_3 caps on both the upper and lower sides were loaded into the BP insertion holes.

In this study, we assumed a 360-day reactor operation period. All control rods were assumed to be pulled out. The time steps in the burn-up simulations were taken as 0, 1, 5, 30, 60, 120, 180, and 360 days. For each of the time steps, 6 million neutrons were generated. The statistical errors of the effective multiplication factor and reaction rate were less than 0.1 % in all calculations, which is sufficiently accurate for our discussion.

2.3. Analysis model of T outflow to the He coolant

In the experiment, the pressure of hydrogen in the quartz tube (see Fig. 1) was determined using the following pressure balance equation:

$$\frac{dp(t)}{dt} = \left(S_0 - \frac{dn_{ZrC}(t)}{dt}\right)\frac{RT}{2V_c} \quad (1)$$

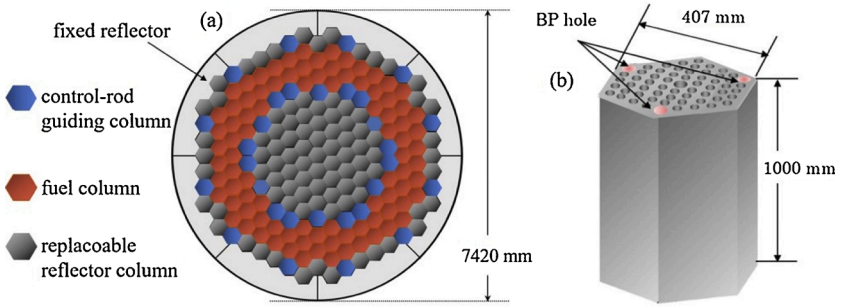

Fig. 2. (a) Horizontal cross-section of the GTHTR300 core; (b) fuel block with BP (Li rod insertion) holes.

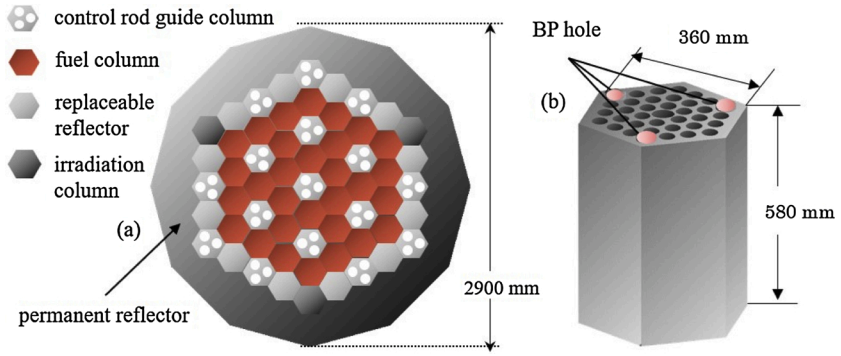

Fig. 3. (a) Horizontal cross-section of the HTTR core; (b) fuel block with BP (Li rod insertion) holes.

where $p(t)$ and $n_{ZrC}(t)$ represent the hydrogen pressure and the number of hydrogen atoms absorbed into the Zr cylinder, respectively, dn_{ZrC}/dt is the hydrogen absorption rate into the Zr cylinder, and S_0 the hydrogen inlet rate, which is controlled by the mass-flow controller (see Fig. 1). R, T, and V_c are the gas constant, temperature, and total volume of the quartz tube, gas tank, and flexible tubes, respectively. Here, to obtain the hydrogen absorption rate, we simultaneously solve the following diffusion equation for the Zr cylinder:

$$\frac{\partial c_{ZrC}(t,r)}{\partial t} = D_{Zr}\frac{1}{r}\frac{\partial}{\partial r}\left(r\frac{\partial c_{ZrC}(t,r)}{\partial r}\right) \tag{2}$$

with the initial and boundary (on the basis of Sieverts' law) conditions, $c_{ZrC}(0,x) = 0$ and $c_{ZrC}(t,x = x_{boudary}) = S_{Zr}p(t)^{1/2}$. The number of hydrogen atoms at t absorbed into Zr, i.e., $n_{Zrc}(t)$, can be estimated by

$$n_{ZrC}(t) = \int_{V_{ZrC}} c_{ZrC}(t,r)d^3r \tag{3}$$

where V_{ZrC} is the volume of the cylindrical Zr absorber.

It should be noted that Eq. (1) can be extended to express the pressure balance in the Li-loading rod in the HTGR core. In such a case, the T inlet speed (S_0) corresponds to the T production rate in a Li-loading rod, which can be evaluated as

$$S_0(t) = \int_{Lirod}\int \Sigma_{n-Li}(\vec{r},E)\phi(t,\vec{r},E)d^3rdE \tag{4}$$

where Σ_{n-Li} represents the ^{6}Li(n,α)T macroscopic cross-section, and ϕ is a neutron flux in the Li-loading region, which is evaluated by the Monte Carlo simulation using the MVP, as described in the previous section, so as to satisfy the critical condition of the reactor. In the reactor, the quartz tube should also be replaced by the dense quality Al_2O_3 cylinder, and, to estimate the amount of T outflow to the He coolant, the diffusion equation for the Al_2O_3 cylinder should be simultaneously solved:

$$\frac{\partial c_{Al}(t,r)}{\partial t} = D_{Al}\frac{1}{r}\frac{\partial}{\partial r}\left(r\frac{\partial c_{Al}(t,r)}{\partial r}\right) \tag{5}$$

with the initial and boundary conditions, $c_{Al}(0,r) = 0$, $c_{Al}(t,r = r_{inside}) = S_{Al}p(t)^{1/2}$, and $c_{Al}(t,r = r_{outside}) = 0$. It has already been confirmed that hydrogen permeates through the Al_2O_3 tube in an atomic form (i.e., the hydrogen concentration is proportional to the square root of an input hydrogen pressure [6]), so we determined the boundary condition of Eq. (5) at the inner surface of the Al_2O_3 tube on the basis of Sieverts' law. The number of T atoms absorbed in the Al_2O_3 at time t, i.e., $n_{Al}(t)$, can be estimated as

$$n_{Al}(t) = \int_{V_{Al}} c_{Al}(t,r)d^3r \tag{6}$$

where V_{Al} is the volume of the cylindrical Al_2O_3 layer. The outflow of T from the outer surface of the Al_2O_3 cylinder into the He coolant was estimated from a nonequilibrium solution of the above T diffusion equation for the Al_2O_3 cylinder as follows:

$$J = -A_{Al}D_{Al}\left.\frac{\partial c_{Al}}{\partial r}\right|_{boundary} \tag{7}$$

where A_{Al} is the outer surface area of the Al_2O_3 cylinder. The diffusivity D_{Al} and solubility S_{Al} coefficients of Al_2O_3 for a hydrogen isotope were drawn from the work of Katayama [6].

To estimate the T absorption rate, Eq. (2) is also solved at the same time. When we consider the T absorption by the Zr pebbles included in the center portion of the Li-loading rod, we can simultaneously solve the diffusion equation for the Zr pebbles in the spherical coordinate:

$$\frac{\partial c_{ZrS}(t,r)}{\partial t} = D_{Zr}\frac{1}{r^2}\frac{\partial}{\partial r}\left(r^2\frac{\partial c_{ZrS}(t,r)}{\partial r}\right) \tag{8}$$

with the initial and boundary conditions, $c_{ZrS}(0,r) = 0$, $c_{ZrS}(t,r = r_{outerside}) = S_{Zr}p(t)^{1/2}$. In the same manner as Eq. (1), the number of T atoms in a Zr

pebble is defined as $n_{ZrS}(t)$:

$$n_{ZrS}(t) = \int_{V_{ZrS}} c_{ZrS}(t,r)d^3r \tag{9}$$

loading rod. The yellow curve corresponds to the T concentration.

In this study, we ignored the function of Zr as an antipermeation material (Zr only exists to absorb the T and keep the pressure at a lower level). This treatment can estimate the T leakage on the safe (larger) side. T produced in the $LiAlO_2$ layer diffuses quickly in the hollow portion, and we assume that the pressure of T in the $LiAlO_2$ and the hollow portion layers reaches the same value (see Fig. 4). Therefore, the pressure balance in the reactor can be written as

$$\frac{dp(t)}{dt} = \left(S_0 - \frac{dn_{ZrC}(t)}{dt} - N_{ZrS}\frac{dn_{ZrS}(t)}{dt} - \frac{dn_{Al}(t)}{dt} + D_{Al}A_{Al}\frac{dc_{Al}(t,r)}{dr}\bigg|_{boundary}\right)\frac{RT}{2V_p} \tag{10}$$

where V_p is the sum of the volumes of the hollow portion (without Zr pebbles) and porosity in the $LiAlO_2$ layer (see Fig. 4). N_{ZrS} represents the number of Zr pebbles, which is determined from the volumes of both the central hollow portion and the Zr pebbles and their filling ratio. The above time-dependent, non-linear differential equations, i.e., Eqs. (2)–(10), are solved simultaneously, satisfying the T mass balance in the GTHTR300 and HTTR cores, along with the neutron transport and nuclear burning equations to satisfy the reactor criticality condition. The porosities of Al_2O_3 and the $LiAlO_2$ layers are assumed to be 0 and 37 %, respectively, and the filling ratio of the Zr pebbles is 54 %.

3. Results and discussion

3.1. Measurement of basic hydrogen absorption properties of Zr

Fig. 5 illustrates the time variation of the pressure in the quartz tube for several inlet speeds (see Fig. 1). The red circles, green squares, blue triangles, and black diamonds represent the measured data for the inlet speed of 20, 10, 5, and 2.5 sccm, respectively. The red diamonds are the measured data when the Zr cylinder does not exist in the quartz tube for 2.5 sccm inlet speed. The error bars represent the standard deviation. In the viewgraph, it can be seen that the fraction of hydrogen absorption to inlet one increases as the inlet speed decreases. The solid lines denote the result of the simulations. In the simulation, we choose the diffusivity $D = 2.6 \times 10^{-9}$ m^2/s and solubility S =108 mol/m^3/Pa$^{1/2}$ of the Zr to reproduce the measured data. The values of diffusivity and solubility are somewhat smaller but seem to be within the consistent range compared with the previously reported data [16–19].

Next, we look at how the hydrogen absorption property of Zr

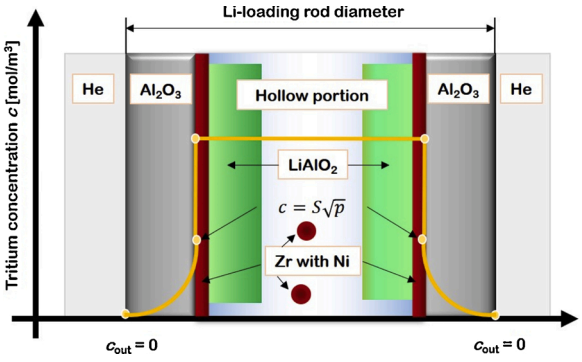

Fig. 4. Conceptual diagram of the T diffusion model in a Li-loading rod. The yellow curve corresponds to the T concentration.

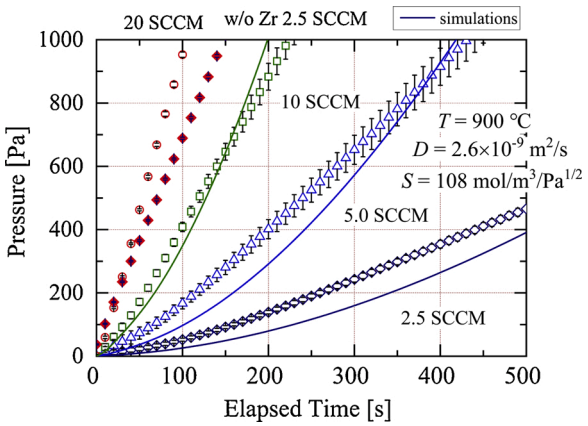

Fig. 5. Comparison between experiment and simulation. Temporal behavior of the pressure in the cylindrical quartz tube for several hydrogen inlet speeds.

depends on the preabsorbed (contained) hydrogen status in the Zr cylinder. We terminated the hydrogen inlet after the pressure had increased to 1,600 Pa. The decrease in pressure after the termination is illustrated in Fig. 6 for several inlet speeds. Until the pressure reached 1,600 Pa, the time duration was almost inversely proportional to the inlet speed, which implies that almost the same number of hydrogen atoms is involved in the Zr cylinder when the inlet is terminated, not depending on the inlet speed. Fig. 6 illustrates the difference in hydrogen absorption speed, in spite of the number of hydrogen atoms involved in the Zr cylinder being almost the same. This is because the gradient of the hydrogen density in the Zr cylinder differs depending on the inlet (absorption) speed. The simulations explain the experiment.

The hydrogen absorption property of Zr also depends on the quantity of preabsorbed T. The temporal pressure decrease after termination of the inlet is plotted in Fig. 7 for several different initial pressures. The dotted lines represent the least-square fitting for an exponential function. In the experiment, the quantity of preabsorbed hydrogen grew large as the initial pressure increased. It was found that as the preabsorbed hydrogen increased, the absorption speed decreased. From the fitting lines, we could estimate based on the absorption times that the pressure decreased to $1/e$ from the initial values, i.e., 6.75, 9.93, and 12.4 s for 400, 800, and 1,600 Pa initial pressures.

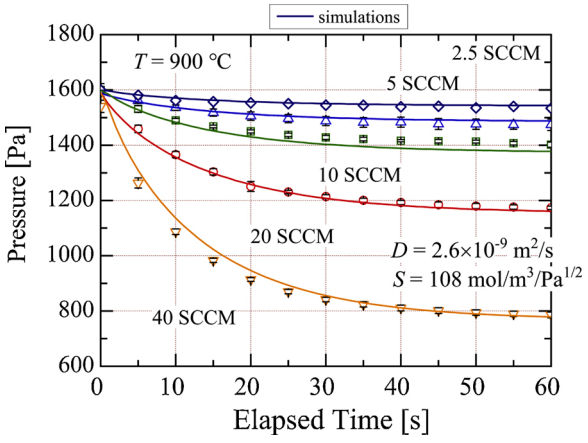

Fig. 6. Comparison between experiment and simulation. Temporal behavior of the pressure in the cylindrical quartz tube after termination of the hydrogen inlet at 1,600 Pa for several inlet speeds.

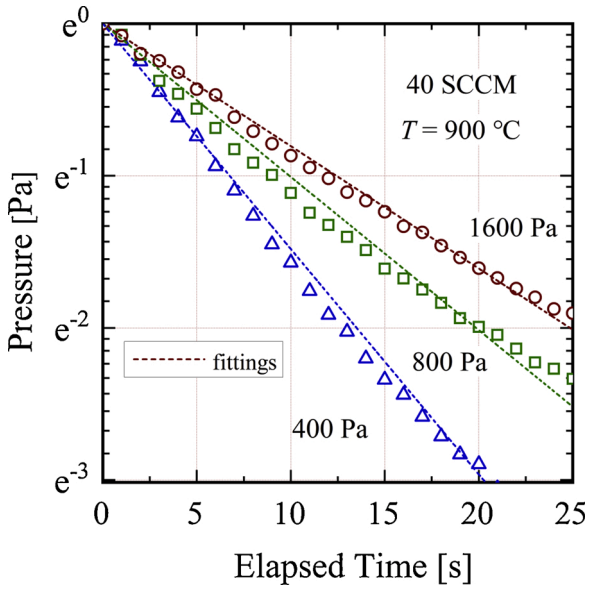

Fig. 7. Temporal behavior of the decreased hydrogen pressure in the cylindrical quartz tube due to absorption by Zr after reaching 400, 800, and 1,600 Pa hydrogen pressure.

3.2. Estimation of the T outflow to the He coolant in the GTHTR300 and HTTR

In this section, we estimate the T outflow from the Li rod to the He coolant during the 360-day operations of the GTHTR300 and HTTR used in this study. Throughout the simulations, we assumed the Li-loading rod structures as indicated in Table 2. When we used the porosities of Al_2O_3, the $LiAlO_2$ layers, and filling ratio of the Zr pebbles presented above, the cumulative weight of the amount of produced T was estimated to be ~610 (~30) g for GTHTR300 (HTTR). The properties of the Li-loading rods in the GTHTR300 and HTTR are listed in Table 2.

The amount of T outflow from the Li-loading rods for GTHTR300 and HTTR was evaluated by simultaneously solving Eqs. (2)–(10). With Eq. (7), the weight of T flowing out from all rods was estimated. From eqs. (3), (6), and (9), the amount of T existing in the Zr and Al_2O_3 layer can also be evaluated. From the pressure $p(t)$, the amount of T_2 gas existing in a hollow portion and property of the $LiAlO_2$ layer is obtained, in accordance with the ideal gas equation. The weights of T existing in Zr, Al_2O_3, the hollow portion, the $LiAlO_2$ layers, and the outflow into the He coolant are presented in Fig. 8 as functions of the reactor operation time for (a) GHTTR300 and (b) HTTR. The temperature was assumed to be 900 °C. In the simulations, the diffusivity $D = 2.6 \times 10^{-9}$ m^2/s and solubility S =108 $mol/m^3/Pa^{1/2}$ of the Zr are assumed. The bold black lines show the cumulative weight of T produced in the reactor $M(t)$, which is calculated as

Table 2
Design parameters of the Li-loading rods for the GTHTR300 and HTTR.

	GTHTR300	HTTR
Electric output [MW]	300	—
Thermal output [MW]	600	30
Height [mm]	950	450
Li rod diameter [mm]	44	14
Inner radius [mm]		
Al_2O_3 layer	15.6	5.2
Zr layer (/w Ni)	14.6	5.0
$LiAlO_2$ layer	12.2	2.3
Zr pebbles with Ni coating [mm] radius	0.5	0.5

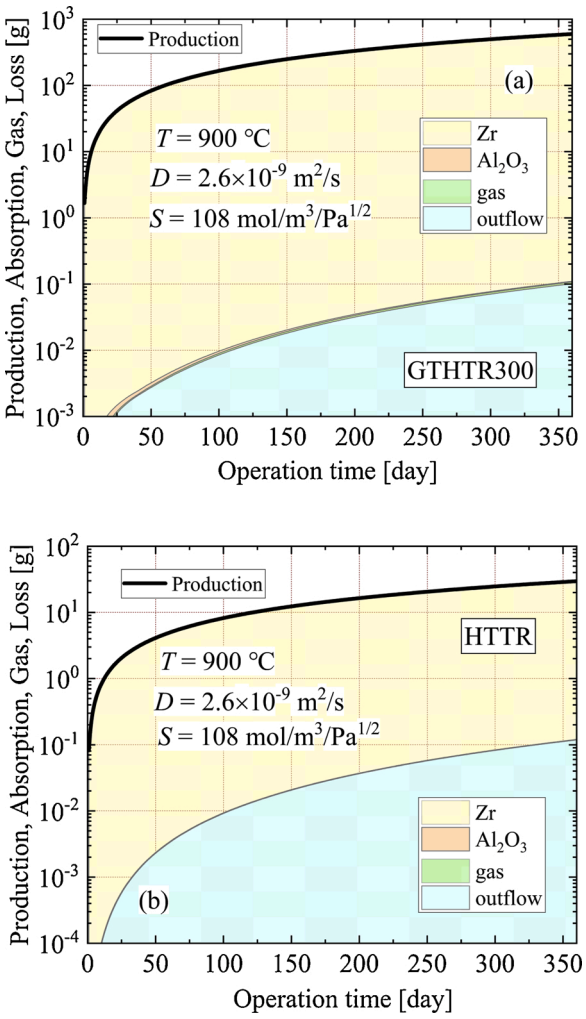

Fig. 8. Temporal behavior of the cumulative weights of T produced, absorbed in the Zr and Al_2O_3 layers, remains as T_2 gas and is flown out of the Li-loading rods in the (a) GTHTR300 and (b) HTTR cores. The diffusivity ($D = 2.6 \times 10^{-9}$ m^2/s) and solubility (S =108 $mol/m^3/Pa^{1/2}$) for Zr were adopted for the simulations.

$$M(t) = \int_o^t S_0(t')dt' \tag{11}$$

We confirmed that the sum of weights, i.e., T in Zr, the Al_2O_3 layers, the hollow portion, and outflow, agreed with $M(t)$. If the Zr properties measured in our experiment were retained during reactor operation, the outflow T can be estimated at less than 0.1 % (0.5 %) for GTHTR300 (HTTR) after 360 days of operation. The total production of T was 610 (30) g for GTHTR300 (HTTR), so the weight of outflow T was almost 0.5 (0.15) g. In standard HTGRs, T is always produced by the ternary fission reaction of fuel particles, with reactions between neutrons and impurities contained in the core graphite, e.g., ^{6}Li, in the helium coolant; ^{3}He, in the control rod; and ^{10}B, even if we do not artificially load the ^{6}Li into the core [20]. The natural weight of T generation in GTHTR300 (HTTR) was estimated at ~20 (0.24) g per year [21]. The evaluated T outflow was at a lower level compared with that in the natural generation.

In the HTGR, a large core size made it possible to load a significant amount of Zr into the Li rod. The atomic ratio T/Zr could be estimated to be less than 0.1 at most, even after the 360-day operation. In such a case, as was shown by Zuzek [22], the capability of T absorption in Zr would be sufficiently high to reduce the partial T pressure, as long as the ideal condition was satisfied during operation. In the HTGR, the T absorption

capability would be reduced by oxidization through interaction with coexisting oxides (i.e., $LiAlO_2$ and Al_2O_3). To prevent such a deterioration, coating with an antioxidant material is necessary [7]. Accordingly, we coated the Zr with Ni. In this case, the T absorption property was reduced. In our study of a cooperative project, the decrement was experimentally ascertained [23], and it was predicted that the diffusivity was determined from the Ni property, so the diffusivity was reduced by ~1/2,000 from that of the previously reported values. Yamanaka [24] reported that the relative reduction in solubility due to oxidization was restricted to 1/3–1/2 in the HTGR condition when the O/Zr atomic ratio was within 0.25–0.398. In our experiments, the significant deterioration in the solubility was also not observed.

To examine the degree of deterioration at which the diffusivity and solubility induces an increment of the outflow ratio larger than 1% of the total T production, simulations were made that assumed a solubility of 1/100 (1/10), in addition to the deterioration of diffusivity of 1/2,000 for GTHTR300 (HTTR). In the current Li-rod design (see Table 2) the Zr/T atomic ratio is much larger in the GTHTR300 than in the HTTR. This is the reason why the reduction in the solubility (to reach the outflow ratio above 1%) is different in the two devices in Fig. 9. The results are displayed in Fig. 9 for (a) GTHTR300 and (b) HTTR. For GTHTR300, when the diffusivity $D = 1.3 \times 10^{-12}$ m^2/s and solubility S =1.08 $mol/m^3/Pa^{1/2}$ are assumed, the T outflow ratio reaches 1.6 % (~10 g), which is still smaller in comparison to natural production.

4. Concluding remarks

In this paper, we described an analytical model for evaluating T leakage from an Li rod and for developing a suitable rod structure. On the basis of this model, T outflow from the rods was estimated using the measured diffusivity and solubility of Zr, assuming GHTR300 and HTTR. By utilizing the Ni-coated Zr in the Al_2O_3 cylinder, the T outflow could be suppressed to less than 1% of the T produced in both reactors. If the solubility deteriorated by 1/100 (1/10) from the measured value, in addition to the deterioration in the diffusivity (1/2,000), the outflow ratio would reach 1.6 (4.0)% to the weight produced ~610 (~30) g during 360 days of operation in GTHTR300 (HTTR).

We are currently planning an irradiation test of the Li-loading rod (demonstration of T production), using HTTR, in the near future. In the first stage of the irradiation test we will use a smaller-size test module to suppress the large amount of T production. The present model would be a tentative proposal for discussion. By comparing the predicted values with the measured data, the presented model could be improved. If the T outflow ratio increases, modification of the Li-loading rod structure would be necessary, i.e., an increment in the quantity of Zr and/or Al_2O_3 in a Li rod would be entailed. In this paper, we have considered containment of T in the Li rod. As another option, a continuous T recovery system contained in the He gas could be considered in future research [25]. Ongoing discussion is important.

Throughout the discussion, we have ignored the antipermeation property of the Zr. In our study of a cooperative project, another experiment using the Zr as an antipermaeation material has also been progressed; and good performance was reported [9,17,26]. This may further improve the T containment performance in HTGRs, and the reflection of the results to the design of the Li-loading rod structure is expected.

To recover the T from the Li rod after the HTGR operation, we must increase the temperature of the Li rods in a considerably high vacuum state [27]. To recover the remaining small amount of T, the Li rods might be dissolved in concentrated hydrochloric acid [28–30].

Declaration of Competing Interest

In the fusion reactor development, establishment of the tritium supply scenario is required for initial startup of DEMO reactor and prior engineering test of the reactor system with tritium circulation. We are considering the tritium supply using the high-temperature gas-cooled reactor (HTGR). This is a first attempt in the world. The HTGR has a unique reactor core structure, and which has attractive and profitable features as a tritium production device. We are currently planning an irradiation test of the tritium production using HTGR in 2022 at the earliest. In this paper, we show a tentative analysis model to analyze the tritium production rate and outflow rate from the Li-loading rods to the He coolant, considering the criticality in the fission reactor nuclear burning. We believe that the development of the system would provide many useful knowledges to the fusion community.

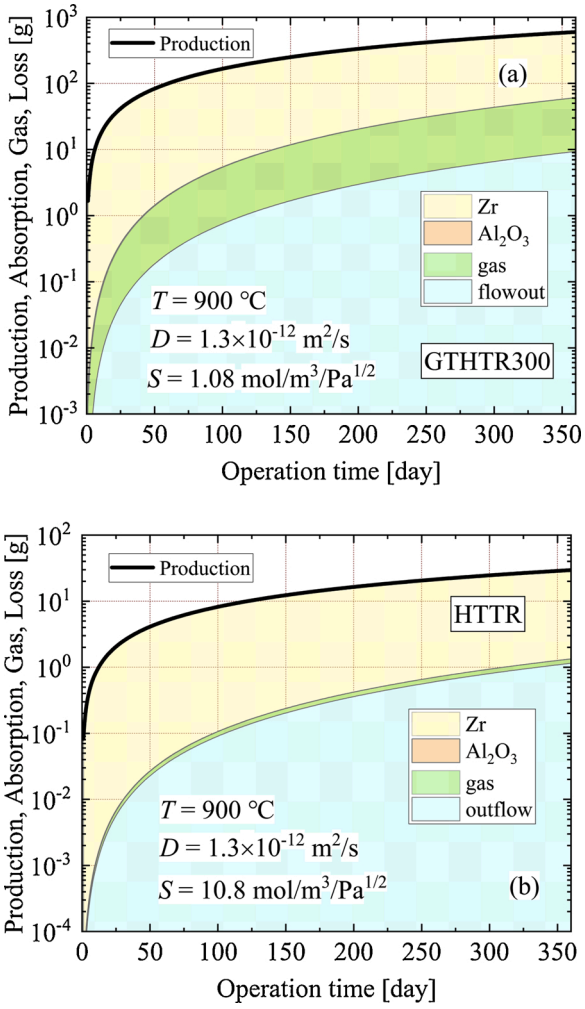

Fig. 9. Temporal behavior of the cumulative weights of T produced, absorbed in the Zr and Al_2O_3 layers, remains as T_2 gas and flows out of the Li-loading rods in GTHTR300 and (b) HTTR cores. The diffusivity ($D = 1.3 \times 10^{-12}$ m^2/s) and solubility (S = 1.08 (10.8) $mol/m^3/Pa^{1/2}$ for Zr in the GTHTR300 (HTTR) were adopted for the simulations.

Acknowledgments

This work was supported by JSPS (Japan Society for the Promotion of Science) KAKENHI Grant-in-Aid for Scientific Research (B) JP18H1200 and cooperative program with BA (The Joint Implementation of the Broader Approach Activities in the Field of Fusion Energy Research) reactor design team in Japan.

References

[1] M. Nishikawa, H. Yamasaki, H. Kashimura, S. Matsuda, Effect of outside tritium source on tritium balance of a D-T fusion reactor, Fusion Eng. Des. 87 (2012) 466–470.

[2] P. Gierszewski, Tritium supply for near-term fusion devices, Fusion Eng. Des. 10 (1989) 399–403.
[3] H. Matsuura, S. Kouchi, H. Nakaya, et al., Performance of high-temperature gas-cooled reactor as a tritium production device for fusion reactors, Nucl. Eng. Des. 243 (2012) 95–101.
[4] M. Goto, K. Okumura, S. Nakagawa, et al., Nuclear and thermal feasibility of lithium-loaded high temperature gas-cooled reactor for tritium production for fusion reactors, Fusion Eng. Des. 136 (2018) 357–361.
[5] H. Nakaya, H. Matsuura, K. Katayama, et al., Study on a method for loading a Li compound to produce tritium using high-temperature gas-cooled reactor, Nucl. Eng. Des. 292 (2015) 277–282.
[6] K. Katayama, H. Ushida, H. Matsuura, et al., Evaluation of tritium confinement performance of alumina and zirconium for tritium production in a high-temperature gas-cooled reactor for fusion reactors, Fusion Sci. Tech. 68 (2015) 662–668.
[7] K.A. Burn, E.F. Love, C.K. Thornhill, Description of the Tritium-Producing Burnable Absorber Rod for the Commercial Light Water Reactor, TTQP-1-015, 19, PNNL, 2012, p. 22086.
[8] S. Nagasumi, H. Matsuura, K. Katayama, et al., Study on tritium production using a high-temperature gas-cooled reactor for fusion reactors: evaluation of tritium outflow by non-equilibrium diffusion simulations, Fusion Sci. Tech. 72 (2017) 753–759.
[9] K. Katayama, J. Izumino, H. Matsuura, S. Fukada, Evaluation of hydrogen permeation rate through zirconium pipe, Nucl. Mater. Energy 16 (2018) 12–18.
[10] Y. Koga, H. Matsuura, Y. Ida, et al., Study on Lithium rod test module and irradiation method for tritium production using high temperature gas-cooled reactor, Fusion Eng. Des. 136 (2018) 587–591.
[11] H. Matsuura, R. Okamoto, Y. Koga, et al., Li-rod structure in high-temperature gas-cooled reactor as a tritium production device for fusion reactors, Fusion Eng. Des. 146 (2019) 1077–1081.
[12] T. Nakata, S. Katanishi, S. Takada, et al., Nuclear Design of the Gas Turbine High Temperature Reactor (GTHTR300), JAERI-Tech, 2002, 2002-066.
[13] S. Saito, T. Tanaka, Y. Sudo, et al., Design of High Temperature Engineering Test Reactor (HTTR), JAERI, 1994, p. 1332.
[14] Y. Nagaya, K. Okumura, T. Mori, M. Nakagawa, MVP/GMVP II: General Purpose Monte Carlo Codes for Nuetron and Photon Transport Calculations Based on Continuous Energy and Multigroup Methods, JAERI, 2005, 1348.
[15] K. Shibata, O. Iwamoto, T. Nakagawa, et al., JENDL-4.0: a new library for nuclear science and engineering, J. Nucl. Sci. Tech. 48 (2011) 1–30.
[16] M. Nagasaka, T. Yamashina, Solubility of hydrogen and deuterium in titanium and zirconium under very low pressure, J. Less-Common Metals 45 (1976) 53–62.
[17] J. Izumino, K. Katayama, H. Matsuura, et al., Study on hydrogen absorption in Zr power used for tritium confinement in a production system of tritium for fusion reactors with a high-temperature gas-cooled reactor, Nucl. Mater. Energy 17 (2018) 289–294.
[18] W.M. Albrecht, W.D. Goode, The Diffusion of Hydrogen in Beta Zirconium, BMI-1373, 1959, https://doi.org/10.2172/4247005.
[19] M. Someno, Solubility and diffusion of hydrogen in zirconium, J. Jpn. Inst. Met. 24 (1960) 249–253 (in Japanese).
[20] B.W. Gainey, A review of tritium behavior in HTGR system, GA-A13461, General Atomic (1976), https://doi.org/10.2172/7359491.
[21] H. Ohashi, N. Sakaba, T. Nishihara, et al., Analysis of tritium behavior in very high temperature gas-cooled reactor coupled with thermochemical iodine-sulfur process for hydrogen production, J. Nucl. Sci. Tech. 45 (2008) 1215–1227.
[22] E. Zuzek, J.P. Abrlata, A. San-Martin, F.D. Manchester, The H-Zr (Hydrogen-Zirconium) system, Bull. Alloy Phase Diag. 11 (1990) 385–395.
[23] T. Otsuka, S. Yokoyama, Y. Akahoshi, et al., T-containment performance of Li rod in High-temperature gas-cooled reactor for T production: (1) hydrogen absorption properties of Ni coated zircaliy-4 Co-existing with Li oxide, AESJ Annual Meeting (2020) (in Japanese).
[24] S. Yamanaka, T. Tanaka, M. Miyake, Effect of oxygen on hydrogen solubility in zirconium, J. Nucl. Mater. 167 (1989) 231–237.
[25] H. Matsuura, H. Nakaya, Y. Nakao, et al., Evaluation of tritium production rate in a gas-cooled reactor with continuous recovery system for fusion reactor, Fusion Eng. Des. 88 (2013) 2219–2222.
[26] D. Henzen, K. Katayama, H. Matsuura, Evaluation of tritium confinement performance the aassembly composed of zirconium and alumina simulating lithium rod, Fusion Eng. Des. 168 (2021), 112372.
[27] K. Ashida, Y. Hatano, W. Nishida, et al., Recovery of hydrogen isotopes by Pd-coated ZrNi from inert gas atmosphere containing impurities, J. Nucl. Sci. Tech. 38 (2001) 952–958.
[28] S. Sato, Y. Verzilov, K. Ochiai, et al., Neutronics experimental study on tritium production in solid breeder blanket mockup with neutron reflector, J. Nucl. Sci. Tech. 44 (2007) 657–663.
[29] A. Klix, Y. Verzilov, K. Ochiak, et al., Recent tritium breeding experiments with lithium titanate mock-ups irradiated with DT neutrons, JAERI-Conf 2004-012 (2004) 209–214.
[30] R. Dierckx, Direct tritium production measurement in irradiated Lithium, Nucl. Inst. Methods 107 (1973) 397–398.